Non-localized thermal behavior of rotating micromachined beams under dynamic and thermodynamic loads

Ahmed E. Abouelregal [1,2], Hamid M. Sedighi [3*], Mohammad Malikan [4], Victor A. Eremeyev [4,5,6]

[1] Department of Mathematics, College of Science and Arts, Jouf University, Al-Qurayyat, Saudi Arabia
[2] Department of Mathematics, Faculty of Science, Mansoura University, Mansoura 35516, Egypt
[3] Mechanical Engineering Department, Faculty of Engineering, Shahid Chamran University of Ahvaz, Ahvaz 61357-43337, Iran
[4] Department of Mechanics of Materials and Structures, Faculty of Civil and Environmental Engineering, Gdansk University of Technology, 80-233 Gdansk, Gdansk, Poland
[5] Don State Technical University, Gagarina sq., 1, Rostov on Don 344000, Russia
[6] DICAAR, Università degli Studi di Cagliari, Via Marengo, 2, 09123, Cagliari, Italy

*Corresponding author: hmsedighi@gmail.com, h.msedighi@scu.ac.ir

Abstract

Rotating micromachined beams are one of the most practical devices with several applications from power generation to aerospace industries. Moreover, recent advances in micromachining technology have led to huge interests in fabricating miniature turbines, gyroscopes and microsensors thanks to their high quality/reliability performances. To this end, this article is organized to examine the axial dynamic reaction of a rotating thermoelastic nanobeam under a constant-velocity moving load. Using Eringen's nonlocal elasticity in conjunction with Euler–Bernoulli theory and Hamilton's principle, the governing equations are derived. It is assumed that the nanobeam is affected by thermal load and the boundary condition is simply supported. The Laplace transform approach is employed to solve the partial differential equations. A numerical example is presented to analyze the effects of the nonlocal parameter, rotation speed and velocity of the static moving load on the dynamic behavior of the system. The numerical results are graphically illustrated and analyzed to recognize the variations of field variables. Finally, in some special cases, our results are compared to those reported in the literature to demonstrate the reliability of the current model.

Keywords: Micormachined rotating beams; Nonlocal elasticity theory; Thermoelasticity; Nanobeams; Moving load

1. Introduction

The term "nano" refers to the nanometer scale and, more generally, to clearly sub-micron dimensions. More specifically, nanoscience is the study of basic principles/interactions of molecules and structures ranging from approximately 1 to 100 nanometers. These types of structures are known as nanostructures [1]. The wide range of practical applications in high-tech nano-devises and systems include important nanomaterials in many fields such as aerospace, electronics, automotive, tribology, construction, catalysis, packaging and etc. Other types of nanostructures, for example, nanotubes, nano-plates, and nanobeams were developed due to their advanced applications in electrical equipment and nuclear microscopes.

A result of various aspects of nano realm appears in nanotechnology which involves nanoscience, engineering and technology. Simulation and manipulation of material in the nanoscale regime are part of it. Nanotechnology requires at least one-dimensional creation of miniaturized devices with nanometer dimensions [2]. Different molecular components may also be incorporated into a functional system in nanotechnology. The advantages are thus tangible in the fields of aerospace and defense, energy storage, remediation and restoration, human health and other scientific areas. All recent accomplishments have profoundly altered our quality of life [2]. Microscale plates and beams are the building blocks of biosensors, smartphone’s micro gyroscopes, microscale vibration energy harvesters and microactuators and many other micro-electro-mechanical systems where the operating concept is their time-dependent deformations or movements [3-9].

In recent years, researchers focused on the mechanical characteristics of nanostructures such as nanobeams and plates based on non-classical models of elasticity because of their growing applications in nano-electronic structures and nano-sensors. Non-classical theories such as the theory of nonlocal elasticity [10, 11], strain gradient theory [12] and modified theory of couple stress [13] have been enormously applied to investigate the mechanical features of these structures at the nanoscale. Non-local continuum mechanics are ideal for modeling of nano-sized structures which are based on the size-dependent behavior of such structures in sub-micron scales. A well-known model named modified couple stress theory (MCST) [13] is one of the most common theories in the field. This hypothesis is used to explain the micron-scale size-dependency observations. A new set of equilibrium equations is constructed which is then applied to the idea of the MCST. A novel equilibrium equation for couple stresses is included in this theory. It is stated that with this new equations, the couple stress tensor in MCST is restricted as symmetric, reducing the number of extra elastic material coefficients. The constitutive equations of the model incorporate extra elastic material constants expressing the material's internal characteristic length as a result of the contribution of couple-stresses.

Practical observations on microstructured systems show that the stiffness and strength of materials with a micron and sub-micron dimensions can be greater than their bulk materials and therefore size or scale effects are important for these kinds of materials. The concepts of classical continuum mechanics lack an intrinsic material length scale parameter and hence cannot account for size effects. To overcome this drawback, the nonlocal elasticity theory suggests that the stress field will be non-local because the stress-strain relationship at a given point depends on the strains of the entire medium. As a result, scientists were inspired to create different hypotheses for nonlocal continuum mechanics. The nonlocal theory of elasticity includes a scale-dependent parameter named non-local parameter which provides a mechanism to reduce the rigidity due to the non-local effects [14]. In recent years, several researches were conducted to analyze the elastic, thermal, wave propagation, and vibration behavior of micro- and nano-structures on the basis of various beam theories [15-39].

Nanowires, semi-miniaturized belts, nano-films and silicon-based accelerometers are some examples of axially motion systems utilized in many industries and engineering equipment. In recent decades, therefore, a lot of attention has been paid to mathematical modeling and vibrational analysis of these structures [39, 40]. Within the framework of a generalized non-local thermoelastic approach, Zenkour and Abouelregal [41] studied the dynamic performance and temperature variations of a nano-beam subject to a moving load. The temperature, deflection, displacement and bending moment distributions were calculated using the Laplace transformation technique. Zenkour and Abouelregal [42] examined the dynamic features of a ramp-type heating nanobeam exposed to a moving static load. Arda [43] studied the vibration of an axially loaded viscoelastic nanobeam. Lin and Trethewey [44] investigated the dynamic arbitrary motions of a spring-mass-sweeper device of an elastic beam subject to dynamic loads by employing Euler-Bernoulli beam model. Shariati et al. [45] presented the size-dependent stability analysis of moving viscoelastic functionally graded nanobeams on the basis of nonlocal elasticity theory. Jaiswal and Iyengar [46] considered the dynamic response of an endless long beam resting on a finite depth substrate subject to moving force actions. In the context of Euler-Bernoulli beam theory, Lee [47] studied the transverse vibrations of a beam-type structure in the presence of a static moving load.

Rotating beams are principal components of several micro and nanosystems and devices. In general, some studies of rotating nanobeams were conducted on nano-sized turbines, nanogenerators and nanobots in various machinery and robotic applications. Therefore, it is of great importance for researchers to explore the rotating effects on the overall response of such structures. Rotating beam-type micromachined structures are widely utilized as the blades of microturbines, micromachined gyroscopes, microsensors to measure the angular velocity of a rotating frame and high resolution spinning space miniature structures in small portable micro-satellites and navigation devices. Figure 1 illustrates some realistic applications of miniature rotating beams in modern tools and devices.

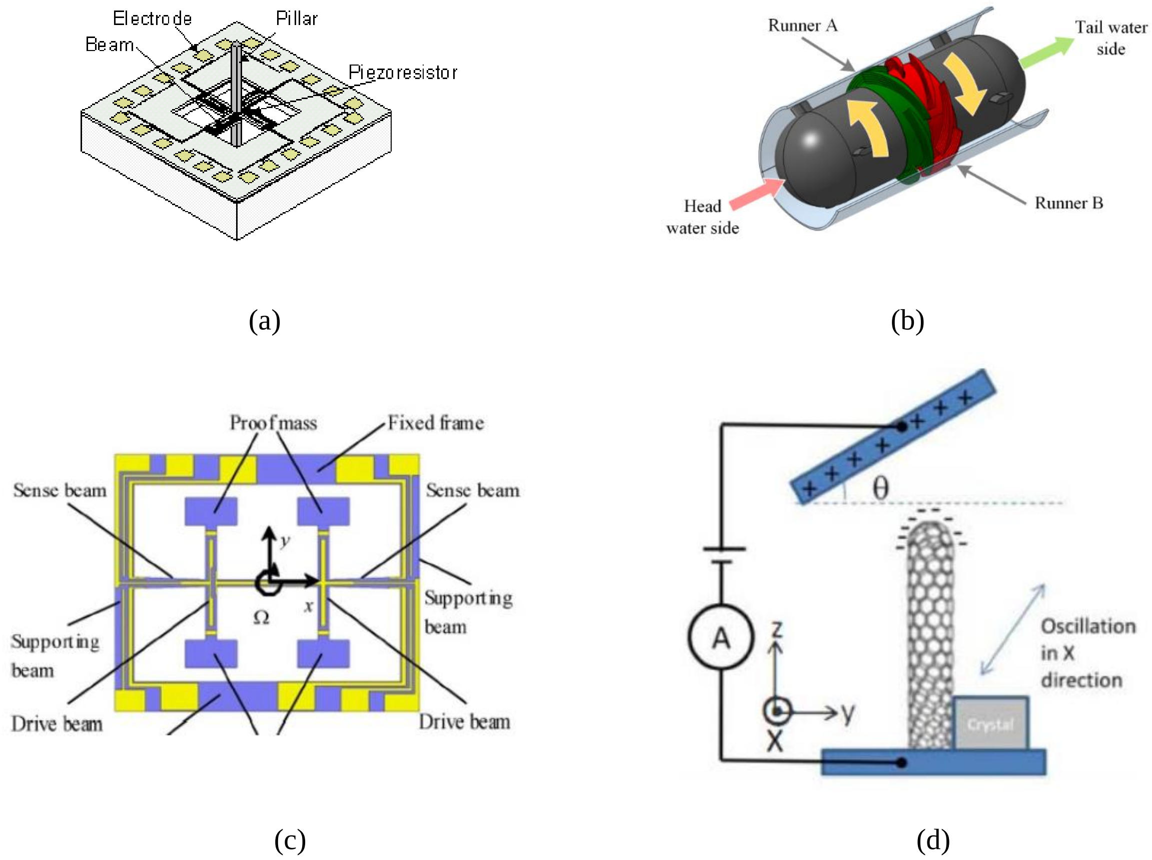

Figure 1: Some realistic applications of rotating micromachined beams (a) microgyroscope with rotary movement of pillars [48] (b) axial microturbine [49] (c) micromachined Gyroscope proposed by National University of Defense Technology (NUDT) [34] (d) Nano-Gyroscope in rotating machine composed of carbon nanotube [50]

Hosseini et al. [51] presented the stress analysis of rotating FGM nano-disks on the basis of strain gradient theory. Mohammadi et al. [52] studied the hygro-mechanical vibration of a spinning, non-linear, nano-viscous beam resting on an elastic visco-Pasternak medium. On the basis of strain gradient theory, Hosseini et al. [53] presented the thermoelastic behavior of rotating FG micro-/nano-disks with variable thickness. In addition, the analysis of smart porous rotating heterogeneous piezo-electric nanobeams was considered by Ebrahimi and Dabbagh [54] within the framework of nonlocal elasticity theory. Khadimallah et al. [55] investigated the impact of three different fraction laws in vibrational behavior of rotating nanostructures. Karimi-Nobandegani et al. [56] studied the instability analysis of rotating cracked beams exposed to tangential compressive loads. Zhang et al. [57] presented the atomistic simulations of double-walled carbon nanotubes on rotational bearings.

Several works in the literature focused on the dynamic characteristics of rotating small-sized structures [58–62] demonstrating the importance of this topic among researchers and scientists.

Geometric nonlinearities are prevalent phenomena in many fields and applications. When the elements are exposed to compressive forces, the stiffness of the structure may be weakened which play a crucial role in the structural performance of the host system and, as a result, it should be considered in the design processes of such systems. Tension forces are seldom a concern since they cause the system's parts to become more rigid. Many structural components may be idealized as beams, such as airplane wings, rotor blades and robot arms. Additionally, the assumption that the unstrained and undeformed configurations are valid at equilibrium state is not always accurate, and the geometrical nonlinearities and deformations must be taken into account. Aeronautics and aerospace fields as well as microelectromechanical systems require models that are more realistic because the physiomechanical characteristics of beam structures play a key role in their optimal design. As a result, modeling of geometrically nonlinearities in such systems is a crucial research topic in the field.

The basic idea of Euler–Bernoulli hypothesis for beams employed in the preceding work is based on the premise that beam deflections are only due to flexural deformations and both rotary inertia and transverse shear effects should be ignored which has acceptable accuracy for several engineering applications. The Timoshenko beam theory, which considers these two factors, gives a better approximation where the thickness of beams are comparable with their lengths. For non-slender beams and high-frequency responses with considerable shear or rotational effects, Timoshenko's beam theory represents a significant improvement. The extra rotation of beam’s cross-section, due to shear deformation, is omitted in Euler-Bernoulli theory. Furthermore, compared to flexural deformation, shear-induced angular distortion is deemed to be minimal. The thin beam theory can be applied to beams in which their lengths are at least 10 times greater than their thicknesses.

The general thermoelasticity theories have been established to resolve the infinite speed of heat waves estimated by the conventional coupled dynamic thermoelasticity models introduced by Biot [63]. Lord and Shulman [64] developed a generalized theory of thermoelasticity by suggesting a novel model to change the conventional Fourier assumption. The vector of heat flux, time derivative and relaxation time were included in this model. Tzou [65-67] considered the influences of infinitesimal interactions in the fast transition operation of a thermal medium within a macroscale framework of two-phase-delay heat conduction (DPL) theory. In a constitutive relationship concerning the heat-wave and temperature changes, two separate phase-lags (one for temperature change and the other for heat-flow vector) were added [68–73]. In realistic engineering applications, the elastic bodies like nanobeams are often subject to variable-temperature ambient, and therefore, the variation of temperature fields should considered. The generalized thermoelasticity theories take into account the relation between temperature and strain rates. The corresponding relations are, furthermore, stated in the form of a hyperbolic function. The contradiction of the high speeds of propagating thermal waves is therefore ignored in the classical coupling model of thermoelasticity.

Because of the widespread use of microbeams in electrical and aerospace engineering as well as the discrepancy between the reference and operating temperatures, it is critical to consider the thermal effects in designing the complex systems with sensitive applications. Few studies have been yet found on the effect of variable temperature of rotating nanobeams in the context of generalized thermoelasticity theory. It should be pointed out that the thermal stresses is one of the most important aspects of spinning micro-beams subject to varying heat sources. Therefore, both thermal and rotating effects should be taken into consideration in order to perform an accurate thermal analysis of such structures.

Based on the mentioned concepts, a thorough investigation on the thermomechanical behavior of a rotating nanobeam influenced by a moving load has been introduced. Furthermore, a system of differential equations for nonclassical nanobeams under a moving mechanical load is established. The constructed model is based on the thermoelastic heat conduction theory with phase lags. Nonlocality and rotational effects on thermoelastic characteristics of the studied problem are considered. The

Laplace transform approach is then exploited to deal with the governing equations. The effects of moving load and the ramp time parameter are also addressed and discussed. The results obtained in this research are compared with the previous models and good agreements are found which demonstrates the accuracy of the present model.

2. Basic equations and problem formulation

The Hamiltonian principle is used to construct the governing equations of the presented model. The fundamental equation based on this principle is given by [21]

$$\delta(U_s + V_e - K_e) = 0 \tag{1}$$

where U_s is the strain energy, V_e is the virtual work due to external forces and K_e is the kinetic energy.

The virtual strain energy δU_s may be defined as [26]

$$\delta U_s = \iint_V \sigma_{ij}\delta\varepsilon_{ij} dV = \iint \sigma_x \delta\varepsilon_{xx} dA dx \tag{2}$$

in which A and L are the cross-sectional area and beam's length. In addition, σ_{ij} and ε_{ij} are, respectively, the stress and the strain tensors which are given by [25, 36]

$$\sigma_{ij} = 2\mu\varepsilon_{ij} + [\lambda\varepsilon_{kk} - \gamma\theta]\delta_{ij}, \tag{3}$$

$$\varepsilon_{ij} = \frac{1}{2}\left(u_{j,i} + u_{i,j}\right) \tag{4}$$

where, λ and μ stand for the Lame's parameters, $\theta = T - T_0$ is the temperature change, T_0 represents the reference temperature, $\gamma = \frac{E\alpha_t}{1-2\nu}$, α_t symbolizes the thermal expansion factor, E denotes the modulus of elasticity and δ_{ij} is the Kronecker's delta function. It is worth mentioning that Lame's parameters are expressed in the following forms [36]:

$$\lambda = \frac{E\nu}{(1+\nu)(1-2\nu)}, \quad \mu = \frac{E}{2(1+\nu)}. \tag{5}$$

As mentioned earlier, the considered nanobeam is subjected to a moving mechanical load. The dimensions of the uniform nanobeam are: length, L $(0 \le x \le L)$ width b $(-b/2 \le y \le +b/2)$ and thickness h $(-h/2 \le z \le +h/2)$. The system is supposed to be initially free of any stress and strain and the initial temperature of the entire beam is T_0 .

According to the assumption of Euler–Bernoulli beam theory with small strains, the non-zero deflections and strains are given by [27, 28]

$$u = -z\frac{\partial w}{\partial x}, v = 0,\ w(x,y,z,t) = w(x,t)$$
$$\varepsilon_{xx} = e = z\frac{\partial^2 w}{\partial x^2} \tag{6}$$

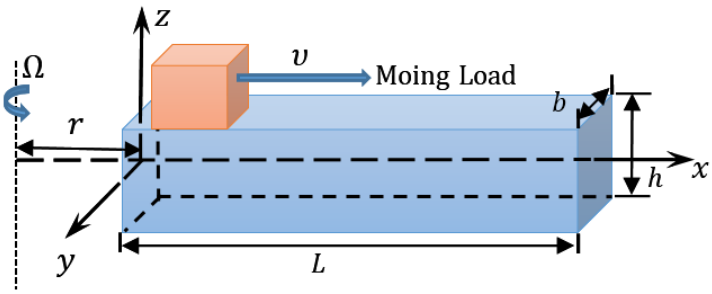

Figure 2: Schematic view of a rotating nanoscale beam subject to a moving load

Therefore, the nonvanishing constitutive relation is expressed as [34]

$$\sigma_x = E\frac{\partial u}{\partial x} - \alpha_T E\theta = -Ez\frac{\partial^2 w}{\partial x^2} - E\alpha_T\theta \tag{7}$$

By inserting Eq. (6) into Eq. (2), the energy of the strain can be calculated as [21, 26]

$$\delta U_s = -\int_0^L M \frac{\partial^2 \delta w}{\partial x^2} dx \tag{8}$$

where the bending moment M is defined by [41, 42]

$$M = \int z\, \sigma_x dA \tag{9}$$

The whole system is rotating around the z-axis with the angular velocity of Ω, therefore, the longitudinal force R should be taken into consideration. Furthermore, if the beam carries a moving load or a particle $q(x,t)$, the virtual potential energy δV_e is defined as follows [47]

$$\delta V_e = -\int_0^L (q-R) \frac{d\delta w}{dx} \frac{dw}{dx} dx \tag{10}$$

Excluding the rotary inertia, the virtual kinetic energy δK_e is given by [47]

$$\delta K_e = \int_0^L \rho A \frac{\partial^2 w}{\partial t^2} \delta w dx \tag{11}$$

Then, one has

$$\int_0^L \left(M \frac{\partial^2 \delta w}{\partial x^2} + (R-q) \frac{d\delta w}{dx} \frac{dw}{dx} + \rho A \frac{\partial^2 w}{\partial t^2} \delta w \right) dx \tag{12}$$

with arbitrary δw over the interval $0 \le x \le L$ and using the integration by parts, the governing equation of motion can be extracted as [50, 51]

$$\frac{\partial^2 M}{\partial x^2} = \frac{\partial}{\partial x}\left[(R-q) \frac{\partial w}{\partial x} \right] + \rho A \frac{\partial^2 w}{\partial t^2} \tag{13}$$

3. Nonlocal elasticity theory

In this section, the non-local elasticity theory [10, 11, 74-77] is used to introduce the small-scale effects in nanoscale beams. From the nonlocal elasticity point of view, the fundamental concept is that the stress in a certain point is not only defined as a function of its own strain but also is affected by the strain fields of all other points of a flexible body. This non-classical theory includes the spatial integration, which is a weighted average of the strain field of the entire body to estimate the stress field. The non-local stress τ_{ij} for any point $\boldsymbol{x}$ of the elastic beam is written by

$$\tau_{ij}(\boldsymbol{x}) = \int_V \Upsilon(|\boldsymbol{x}, \boldsymbol{x}'|, \xi)\, \sigma_{ij}(\boldsymbol{x}') \mathrm{d}V(\boldsymbol{x}') \tag{14}$$

In the above equation, $\Upsilon(|\boldsymbol{x}, \boldsymbol{x}'|, \xi)$ is a positive scalar kernel operator, $\|\boldsymbol{x} - \boldsymbol{x}'\|$ represents the Euclidean distance, $\xi = e_0 a/l$ is the nonlocal scale parameter with the internal and external characteristic lengths of a and l and e_0 is a parameter determined experimentally named the material-dependent constant and δ_{kl} denotes the delta function. When the kernel is chosen as [78, 79]:

$$\Upsilon(|\boldsymbol{x}, \boldsymbol{x}'|, \xi) = \frac{1}{2\pi \xi^2 l^2} K_0 \left(\frac{\|x - x'\|}{\xi l} \right) \tag{15}$$

in which K_0 stands for the modified Bessel function, Eq. (6) can be re-written as:

$$\tau_{ij}(\boldsymbol{x}) - \xi^2 \nabla^2 \tau_{ij} = \sigma_{ij}(\boldsymbol{x}) \tag{16}$$

Eq. (16) is utilized to incorporate the effect of size-dependency in the mechanical behavior of nanostructures.

Using Eq. (3) in (16), the following nonlocal constitutive stress-strain equation can be obtained

$$\tau_{ij} - \xi^2 \nabla^2 \tau_{ij} = 2\mu \varepsilon_{ij} + \lambda \varepsilon_{kk} \delta_{ij} - \gamma \theta \delta_{ij} \tag{17}$$

In one-dimensional analysis, the nonlocal constituent relationships can be summarized as:

$$\tau_{xx} - \xi^2 \frac{\partial^2 \tau_{xx}}{\partial x^2} = -Ez \frac{\partial^2 w}{\partial x^2} - E \alpha_T\, \theta, \tag{18}$$

It is worth noting that by omitting the external characteristic lengths a which means that the elements of the elastic body are assumed to be continuously distributed, the parameter ξ is equal to zero and the constitutive equation given in Eq. (18) turns to the classical case.

The theory of generalized thermoelasticity [52] was formulated in order to eliminate the infinite thermal diffusion velocity paradox which inherently exist in the traditional coupled thermoelasticity theory which is on the basis of Fourier's law by assuming the heat conduction formulation in the form of the parabolic kind. The model proposed by Tzou [65-67] is among those generalized theories. This model includes two parameters indicating the delay times (phase-lags). The generalized heat equation proposed by Tzou's theory is given by

$$\left(1+\tau_\theta \frac{\partial}{\partial t}\right)(K\theta_{,i})_{,i} = \rho C_E \left(1+\tau_q \frac{\partial}{\partial t}\right)\left(\frac{\partial \theta}{\partial t}\right) + \gamma T_0 \left(1+\tau_q \frac{\partial}{\partial t}\right)\left(\frac{\partial e}{\partial t}\right), \tag{19}$$

where ρ, K and C_E denote the density, thermal conductivity of the material and the specific heat at constant strain, τ_θ represents the phase lag of temperature gradient, τ_q stands for the heat flux phase lag and $e = \partial u/\partial x$ incorporates the normal strain.

The following relation is obtained by the substituting Eq. (6) into Eq. (19)

$$\left(1+\tau_\theta \frac{\partial}{\partial t}\right)\left(\frac{\partial^2 \theta}{\partial x^2}\right) + \left(1+\tau_\theta \frac{\partial}{\partial t}\right)\left(\frac{\partial^2 \theta}{\partial z^2}\right) = \frac{\rho C_E}{K}\left(1+\tau_q \frac{\partial}{\partial t}\right)\left(\frac{\partial \theta}{\partial t}\right) - \frac{\gamma T_0}{K}\left(1+\tau_q \frac{\partial}{\partial t}\right)\left(z\frac{\partial^3 w}{\partial t \partial x^2}\right). \tag{20}$$

in which the longitudinal force $R(x)$ originates from the centrifugal effects at location x (see Fig. 2) and can be determined using the following formula [53, 56]

$$R(x) = \int_x^L \rho A \Omega^2 (r+\chi) d\chi \tag{21}$$

As shown in Fig. 2, the parameter r denotes the distance to the left edge of nano-beam from the center of rotation. Note that if $\Omega = 0$, no rotation exists and the centrifugal tension force R will disappear. The centrifugal tension force R is then given by

$$R(x) = \frac{3L\rho A \Omega^2}{6L}[(L-x)(L+2r+x)] \tag{22}$$

Integrating equation (18) along with the thickness of the beam after multiplying the equation by z and then one has

$$M - \xi \frac{\partial^2 M}{\partial x^2} = -EI\frac{\partial^2 w}{\partial x^2} - EI\alpha_T M_T, \tag{23}$$

in which $I = bh^3/12$, EI is the flexural rigidity and M_T is the resulting moment caused by the effect of temperature gradient which is defined by

$$M_T = \frac{12}{h^3}\int_{-h/2}^{h/2} \theta(x,z,t)\, z dz. \tag{24}$$

The following equation can be obtained by substituting Eq. (23) from Eq. (13)

$$M = \xi \rho A \frac{\partial^2 w}{\partial t^2} - \xi(q(x) - R(x)) - EI\frac{\partial^2 w}{\partial x^2} - EI\alpha_T M_T, \tag{25}$$

The governing equation for the rotating nonlocal nano-beam can be obtained using Eq. (13) and (25) in terms of the deflection w as follows

$$\frac{\partial^4 w}{\partial x^4} + \frac{\rho A}{EI}\left(1 - \xi\frac{\partial^2}{\partial x^2}\right)\left(\frac{\partial^2 w}{\partial t^2}\right) + \alpha_T \frac{\partial^2 M_T}{\partial x^2} = \frac{1}{EI}\left(1 - \xi\frac{\partial^2}{\partial x^2}\right)(q(x) - R(x)) \tag{26}$$

Equations (20) and (26) represent the basic equations for nonlocal rotating nanobeams on the basis of dual-phase thermoelasticity model.

4. Solution of the problem

In this work, the temperature change, $\theta(x,z,t)$, in the longitudinal direction of the nanobeam is studied and it is assumed that there is no heat flow through the upper and lower surfaces of the beam, i.e. $\frac{\partial \theta}{\partial x} = 0$ at $z = \pm h/2$. For a very thin beam, it is supposed that the temperature gradient can be described in terms of $\sin(\pi z/h)$ as follows:

$$\theta(x,z,t) = \Psi(x,t)\sin(pz), \quad p = \frac{\pi}{h}. \tag{27}$$

By considering Eq. (27), the governing equations (20), (25) and (26) become

$$\frac{\partial^4 w}{\partial x^4}+\frac{\rho A}{EI}\left(1-\xi\frac{\partial^2}{\partial x^2}\right)\left(\frac{\partial^2 w}{\partial t^2}\right)+\frac{24\alpha_T}{\pi^2 h}\frac{\partial^2\Psi}{\partial x^2}=\frac{1}{EI}\left(1-\xi\frac{\partial^2}{\partial x^2}\right)(q(x)-R(x)). \tag{28}$$

$$M=\xi\rho A\frac{\partial^2 w}{\partial t^2}-\xi(q(x)-R(x))-EI\frac{\partial^2 w}{\partial x^2}-EI\frac{24T_0\alpha_T}{\pi^2 h}\Psi, \tag{29}$$

$$\left(1+\tau_\theta\frac{\partial}{\partial t}\right)\left(\frac{\partial^2\Psi}{\partial x^2}-\frac{\pi^2}{h^2}\Psi\right)=\frac{\rho C_E}{K}\left(1+\tau_q\frac{\partial}{\partial t}\right)\frac{\partial\Psi}{\partial t}-\frac{\gamma T_0\pi^2 h}{24K}\left(1+\tau_q\frac{\partial}{\partial t}\right)\left(\frac{\partial^3 w}{\partial t\partial x^2}\right), \tag{30}$$

In order to simplify the governing equations, the system parameters are introduced in non-dimensional forms which helps us to conduct some comparative studies with the previous works in the literature. The following non-dimensional terms are introduced

$$\begin{gathered}(x',L',u',w',z',h',b')=\eta c(x,L,u,w,z,h,b),\quad (t',t'_0,\tau'_q,\tau'_\theta)=\eta c^2(t,t_0,\tau_q,\tau_\theta),\\ \xi'=\eta^2c^2\xi,\quad \Psi'=\frac{\Psi}{T_0},\quad \{q',R'\}=\frac{A}{EI}\{q,R\},\ M'=\frac{M}{\eta cEI},\ c=\sqrt{\frac{E}{\rho}},\ \eta=\frac{\rho C_E}{K},\end{gathered} \tag{31}$$

Then Eqs. (28)-(30) can be written as (the prime symbols are dropped, for the sake of simplicity)

$$\frac{\partial^4 w}{\partial x^4}+\frac{12}{h^2}\left(1-\xi\frac{\partial^2}{\partial x^2}\right)\left(\frac{\partial^2 w}{\partial t^2}\right)+\frac{24T_0\alpha_T}{\pi^2 h}\frac{\partial^2\Psi}{\partial x^2}=\left(1-\xi\frac{\partial^2}{\partial x^2}\right)(q(x)-R(x)), \tag{32}$$

$$\left(1+\tau_\theta\frac{\partial}{\partial t}\right)\left(\frac{\partial^2\Psi}{\partial x^2}-\frac{\pi^2}{h^2}\Psi\right)=\left(1+\tau_q\frac{\partial}{\partial t}\right)\left(\frac{\partial\Psi}{\partial t}\right)-\frac{\gamma\pi^2 h}{24K\eta}\left(1+\tau_q\frac{\partial}{\partial t}\right)\left(\frac{\partial^3 w}{\partial t\partial x^2}\right), \tag{33}$$

$$M(x,t)=\frac{12\xi}{h^2}\frac{\partial^2 w}{\partial t^2}-\xi(q(x)-R(x))-\frac{\partial^2 w}{\partial x^2}-\frac{24T_0\alpha_T}{\pi^2 h}\Psi. \tag{34}$$

The external moving load $q(x,t)$ is supposed to be concentrated with a constant velocity υ along the beam's longitudinal direction and may therefore be represented as [41, 42]

$$q(x,t)=Q_0\delta(x-\upsilon t) \tag{35}$$

in which Q_0 denotes the load strength that assumed to be constant and $\delta(\cdot)$ is the Dirac function. In the present paper, it is assumed that the angular velocity of the nanobeam is constant and therefore the centrifugal load $R(x)$ acts at its maximum value. The axial centrifugal load R is then given by [53, 55]

$$R_{max}=\int_0^L\rho A\Omega^2(r+x)dx=\frac{1}{2}\rho A\Omega^2 L(2r+L) \tag{36}$$

Therefore, the equation of motion (32) can be represented as

$$\frac{\partial^4 w}{\partial x^4}+\frac{12}{h^2}\left(1-\xi\frac{\partial^2}{\partial x^2}\right)\left(\frac{\partial^2 w}{\partial t^2}\right)+\frac{24T_0\alpha_T}{\pi^2 h}\frac{\partial^2\Psi}{\partial x^2}=\left(1-\xi\frac{\partial^2}{\partial x^2}\right)\left[q-\frac{6L\Omega^2(2r+L)}{h^2}\frac{\partial^2 w}{\partial x^2}\right] \tag{37}$$

The bending moment (34) can also be described as

$$M=\frac{12\xi}{h^2}\frac{\partial^2 w}{\partial t^2}-\xi\left[q-\frac{6L\Omega^2(2r+L)}{h^2}\frac{\partial^2 w}{\partial x^2}\right]-\frac{\partial^2 w}{\partial x^2}-\frac{24T_0\alpha_T}{\pi^2 h}\Psi \tag{38}$$

The nanobeam is supposed to be homogeneous, undeformed and initially at rest. Therefore, the following initial conditions are introduced

$$w(x,t)|_{t=0}=\left.\frac{\partial w(x,t)}{\partial t}\right|_{t=0}=0,\quad \Psi(x,t)|_{t=0}=\left.\frac{\partial\Psi(x,t)}{\partial t}\right|_{t=0}=0, \tag{39}$$

On the other hand, the boundary conditions of the structure at the ends $x=0,L$ are provided as

$$w(x,t)=0,\qquad \frac{\partial^2 w(x,t)}{\partial x^2}=0 \tag{40}$$

In addition, it is assumed that

$$\theta=\theta(z,t)=\theta_0\sin(pz)f(x,t)\qquad \text{at}\quad x=0. \tag{41}$$

in which θ_0 stands for as a constant coefficient and the function $f(x,t)$ is expressed by the following formula:

$$f(x,t)|_{x=0}=\begin{cases}0, & t\le 0,\\ \frac{t}{t_0}, & 0\le t\le t_0,\\ 1, & t>t_0,\end{cases} \tag{42}$$

in which t_0 symbolizes the non-negative ramp-type parameter. Furthermore, the temperature at the second end satisfies the following condition:

$$\frac{\partial\Psi}{\partial x}=0\ ,\quad x=L. \tag{43}$$

5. Laplace transform approach

In order to deal with the governing equations, the Laplace transform method is used to reduce the order of the differential equations by omitting the time derivatives and solving the resulting equation in the Laplace space. By applying the Laplace technique, by assuming zero initial conditions (39), Eqs. (33), (37), and (38), in their transformed cases, are written by:

$$A_0\frac{\mathrm{d}^4\bar{w}}{\mathrm{d}x^4}-A_1\frac{\mathrm{d}^2\bar{w}}{\mathrm{d}x^2}+A_2\bar{w}+A_3\frac{\mathrm{d}^2\bar{\Psi}}{\mathrm{d}x^2}=\bar{g}(s)e^{-\frac{s}{v}x}, \tag{44}$$

$$(1+\tau_\theta s)\left(\frac{\mathrm{d}^2}{\mathrm{d}x^2}-A_4\right)\bar{\Psi}=s\big(1+\tau_q s\big)\bar{\Psi}-A_5 s\big(1+\tau_q s\big)\frac{\mathrm{d}^2\bar{w}}{\mathrm{d}x^2}, \tag{45}$$

$$\bar{M}=-A_0\frac{\mathrm{d}^2\bar{w}}{\mathrm{d}x^2}+A_2\bar{w}-A_3\bar{\Psi}-\frac{\xi\,Q_0}{v}e^{-\frac{s}{v}x}, \tag{46}$$

where

$$\begin{gathered}A_0=1-\frac{6L\Omega^2\xi(2r+L)}{h^2},\quad A_1=\frac{12\xi s^2}{h^2}-\frac{6L\Omega^2(2r+L)}{h^2},\quad A_2=\frac{12\xi}{h^2},\\ A_3=\frac{24T_0\alpha_T}{\pi^2 h},\quad \bar{g}(s)=\frac{Q_0}{v}\left(1-\xi\frac{s^2}{v^2}\right),A_4=\frac{\pi^2}{h^2},\quad A_5=\frac{\gamma\,\pi^2 h}{24K\eta}.\end{gathered} \tag{47}$$

Removing $\bar{\Theta}$ from equations (44) and (45), one gets

$$\left[\frac{\mathrm{d}^6}{\mathrm{d}x^6}-A\frac{\mathrm{d}^4}{\mathrm{d}x^4}+B\frac{\mathrm{d}^2}{\mathrm{d}x^2}-C\right]\bar{w}=\Gamma_1 e^{-\frac{s}{v}x} \tag{48}$$

In which

$$\begin{gathered}A=\frac{A_1}{A_0}+\frac{\phi A_3A_5}{A_0}+A_4+\phi,\ B=\frac{A_2}{A_0}+\frac{A_1}{A_0}(A_4+\phi),\ C=\frac{A_2}{A_0}(A_4+\phi),\\ \phi=\frac{s(1+\tau_q s)}{(1+\tau_\theta s)},\ \ \Gamma_1=\bar{g}(s)((s/v)^2-(A_4+\phi))/A_0.\end{gathered} \tag{49}$$

The solution of $\bar{w}$ can be derived from equation (48) as follows:

$$\bar{w}=\sum_{j=1}^{3}\left(C_j e^{-m_j x}+C_{j+3}e^{m_j x}\right)+C_7 e^{-sx/v} \tag{50}$$

where $C_7=\Gamma_1/((s/v)^6-A(s/v)^4+B(s/v)^2-C)$, m_1^2, m_2^2 and m_3^2 represent the roots of characteristic equation governed by

$$m^6-Am^4+Bm^2+C=0. \tag{52}$$

Similarly, by removing $\bar{w}$ from (44) to (45), the governing equation for $\bar{\Theta}$ yields

$$\left[\frac{d^6}{dx^6}-A\frac{d^4}{dx^4}+B\frac{d^2}{dx^2}-C\right]\bar{\Psi}=\Gamma_2 e^{-\frac{s}{v}x}, \tag{53}$$

where $\Gamma_2=qs^2A_5\bar{g}(s)/(v^2A_0)$. In addition, the solution of Eq. (53) can be expressed as

$$\bar{\Psi}=\sum_{j=1}^{3}\beta_i\left(C_j e^{-m_j x}+C_{j+3}e^{m_j x}\right)+C_8 e^{-sx/v} \tag{55}$$

where

$$\beta_i=\frac{qA_5m_i^2}{(A_4+q)-m_i^2},C_8=\frac{\Gamma_2}{(s/v)^6-A(s/v)^4+B(s/v)^2-C}. \tag{56}$$

By substituting $\bar{w}$ and $\bar{\Theta}$ into equation (46), the solution of bending moment $\bar{M}$ is given by:

$$\bar{M}=-\sum_{i=1}^{3}\ (A_0m_i^2-A_2+A_3\beta_i)(C_i e^{-m_i x}+C_{i+3}e^{m_i x})+C_9 e^{-\frac{s}{v}x}, \tag{58}$$

in which

$$C_9=-(A_0(s/v)^2-A_2)C_7-A_3C_8-\frac{\xi\,Q_0}{v} \tag{59}$$

The axial displacement $\bar{u}$ also takes the following form by considering Eqs. (6) and (50)

$$\bar{u}=-z\frac{d\bar{w}}{dx}=z\sum_{i=1}^{3}m_i(C_i e^{-m_i x}-C_{i+3}e^{m_i x})\ \ +(s/v)C_7 e^{-sx/v}. \tag{60}$$

One can obtain the strain field of the nanobeam as

$$\bar{e}=\frac{d\bar{u}}{dx}=-z\ \sum_{i=1}^{3}m_i^2(C_i e^{-m_i x}+C_{i+3}e^{m_i x})\ \ -(s/v)^2C_7 e^{-sx/v}. \tag{61}$$

The boundary conditions (40)-(43) are reduced into the Laplace transform field as

$$\bar{w}(x,s)|_{x=0,L} = 0, \qquad \left.\frac{d^2\bar{w}(x,s)}{dx^2}\right|_{x=0,L} = 0, \tag{62}$$

$$\bar{\Psi}(x,s)|_{x=0} = \theta_0\left(\frac{1-e^{-t_0 s}}{t_0 s^2}\right) = \bar{G}(s). \tag{63}$$

$$\frac{\partial\bar{\Theta}}{\partial x} = 0, \quad x = L. \tag{64}$$

Substitution of Eqs. (50) and (55) into Eqs. (62)-(64) gives

$$\sum_{j=1}^{3}\left(C_j + C_{j+3}\right) = -C_7 \tag{65}$$

$$\sum_{j=1}^{3}\left(C_j e^{-m_j L} + C_{j+3}e^{m_j L}\right) = -C_7 e^{-sL/v} \tag{66}$$

$$\sum_{j=1}^{3} m_j^2\left(C_j + C_{j+3}e^{m_j x}\right) = -C_7 s^2/v^2 \tag{67}$$

$$\sum_{j=1}^{3} m_j^2\left(C_j e^{-m_j L} + C_{j+3}e^{m_j L}\right) = -C_7(s^2/v^2)e^{-sL/v} \tag{68}$$

$$\sum_{j=1}^{3}\beta_i\left(C_j + C_{j+3}\right) \;= \bar{G}(s) - C_8. \tag{69}$$

$$\sum_{j=1}^{3}\beta_j m_j\left(-C_j e^{-m_j L} + C_{j+3}e^{m_j L}\right) \;= C_8(s/v)e^{-sL/v}. \tag{70}$$

The final forms of the solutions to all field variables in the Laplace domain are obtained by determining the integral constants C_j. From equations (47)-(52), the unknown constants C_j can be obtained. The current problem is numerically studied based on the Fourier expansion method by employing mathematical software.

6. Inversion of the Laplace transforms

In order to apply the Laplace transform inversion, the Riemann summation approach is employed to achieve the numerical solution of the transversal deflection, stress field and temperature gradient. In this approach, the time domain solution $\mathrm{H}(x,t)$, can be obtained from the Laplace domain result $\bar{\mathrm{H}}(x,\zeta)$ as follows [67]

$$\mathrm{H}(x,t) = \frac{e^{\zeta t}}{2t}Re[\bar{\mathrm{H}}(x,\zeta)] + \frac{e^{\zeta t}}{t}Re\sum_{n=0}^{N}(-1)^n\bar{\mathrm{H}}\left(x,\zeta + \frac{in\pi}{t}\right), \tag{71}$$

in which ζ represents a real number which is larger than all real components of $\bar{\mathrm{H}}(x,t)$, Re is an operator that extracts the real part of each function, and i is the imaginary unit. Numerical calculations demonstrate that for appropriate convergence, ζ should take the value of $4.7/t$.

7. Numerical results

This section focuses on the thermomechanical behavior of heat waves in nanobeams due to varying heat source. A rotating nanobeam subject to a moving load is modeled using the generalized thermoelasticity and nonlocal Euler-Bernoulli beam theories. Silicon (Si) material was taken into account as the main flexible nanobeam. Different physical properties of this kind of material are as follows [41, 42]:

$$\alpha_T = 2.59\times 10^{-6}\mathrm{K}^{-1}, \quad \nu = 0.22, \quad K = 156\ \mathrm{W/(mK)}, T_0 = 293\ K$$
$$E = 169\ \mathrm{GPa}, \ \rho = 2330\ \mathrm{kg/m^3}, \ C_E = 713\ \mathrm{J/(kgK)}, \ \Omega = 0.1,$$
$$t = 0.1\mathrm{sec}, \ L/h = 10, \ b/h = 0.5, \ L = 1, z = h/3.$$

The dimensions of the microscale beam (such as length, width and thickness) are selected in the range of $(1-100)\times 10^{-9}$m. In picoseconds, in the interval $(1-100)\times 10^{-14}$sec, the relaxation parameter τ_0 and the thermal vibration parameter t_0 are also specified at the instant time t. Moreover, the microbeam's length to thickness ratio is taken as $L/h = 10$ and the other variables are assumed to take the values $t = 0.12$, $L = 1$, $r = 0.05$ and $z = h/3$. The nonlocal parameter and the velocity of the moving load are introduced as follows: $\bar{\upsilon}$ $(\bar{\upsilon} = 10^3\,\upsilon)$ and $\bar{\xi}$ $(\bar{\xi} = 10^3\,\xi)$.

7.1 Validation

By ignoring the impact of rotation speed, one can conclude that there is a good agreement with those reported in [41, 42]. Therefore, the impacts of moving load, rotating speed and phase lags are examined in this research. After analyzing the present approach, the vibrational response of the considered problem is explored by assuming different values of systems parameters. The values of the vector fields may be calculated in accordance with the classical theory of elasticity when the non-local parameter $\bar{\xi}$ is zero. In addition, with the assumption of $\tau_q = \tau_\theta = 0$, the values of the physical fields based on the CTE model can be obtained.

7.2 The nonlocality effect

In the first case, the variations of the non-dimensional deflection, axial displacement, temperature gradient and bending moment are investigated for various values of non-local parameter $\bar{\xi}$. Three values for this parameter, namely $\bar{\xi} = 0$, $\bar{\xi} = 1$, and $\bar{\xi} = 3$, are used, and the other parameters like moving load velocity $\bar{\upsilon}$, rotation Ω and the time of ramp t_0 remain constant as $\bar{\upsilon} = 3$, $\Omega = 0.5$ and $t_0 = 0.1$, respectively. The time delays τ_q and τ_θ are equal to $\tau_q = 0.02$, $\tau_\theta = 0.01$.

It is noted that the classical theory can be reached when $\bar{\xi}$ takes the zero value (**CTE** model) and the nonlocal thermoelasticity theory (**NLTE** model) is indicated by assigning positive values for $\bar{\xi}$. The variation of the physical fields of nanobeam versus dimensionless distance *x* are shown in Figures 3-6 for different nonlocal parameter $\bar{\xi}$. The nanobeam responses are obtained at $t = 0.12$. According to the illustrated results, one can find that the nonlocal parameter has considerable effect on all physical fields and the presence of size-dependency cannot be ignored in the thermoelastic response of rotating nanobems in thermal environment.

Figure 3 shows that, at lower values of *x*, the values of thermal deflection w for **NLTE** model is somehow similar to the classical **CTE** model, however, by increasing the distance *x*, a slight deviation is seen in comparison with the classical theory. This phenomenon is similar to that obtained by Abouelregal and Zenkour [42]. Furthermore, the values of deflection based on NLTE model are greater than the CTE theory.

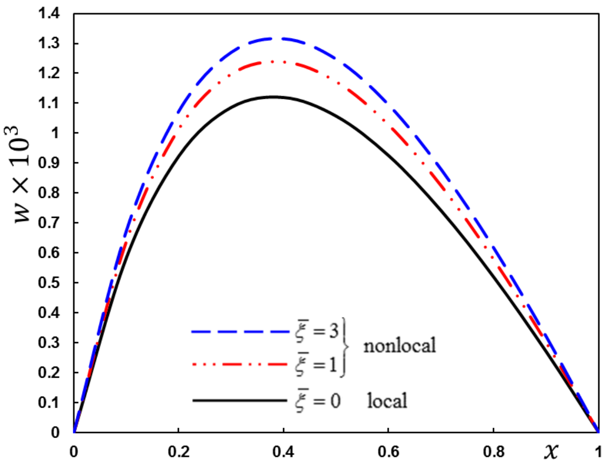

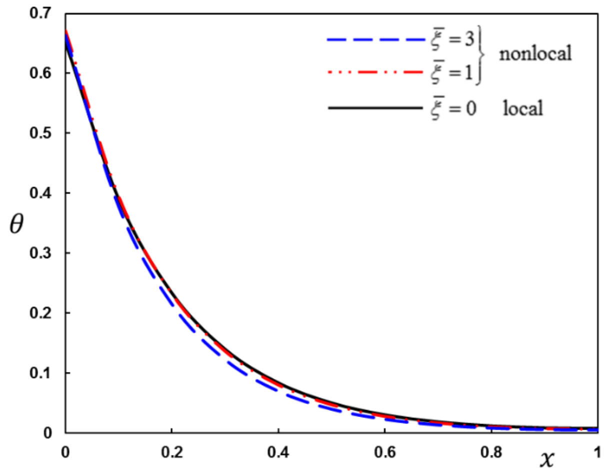

Figure 3: The variation of deflection w vs the nonlocal parameter $\bar{\xi}$

Figure 4: The variation of temperature θ vs the nonlocal parameter $\bar{\xi}$

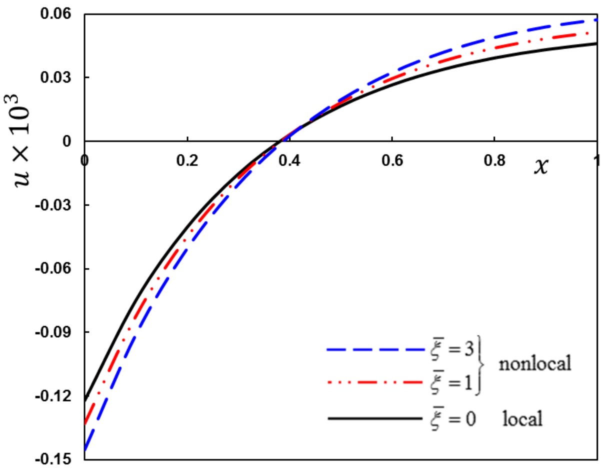

Figure 5: The variation of axial displacement u vs nonlocal parameter $\bar{\xi}$

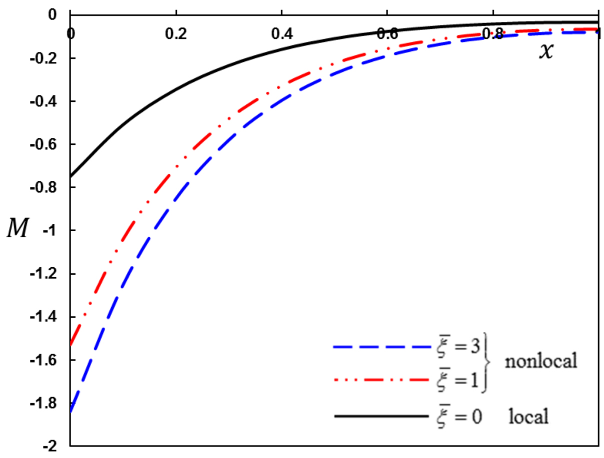

Figure 6: The variation of bending moment M vs nonlocal parameter $\bar{\xi}$

Figure 4 shows the nanobeam thermodynamic temperature θ versus the axial position x in view of some assigned values of $\bar{\xi}$ as 0, 1 and 3. As the distance x increases, the results show that temperature θ decreases against the wave propagation. According to this figure, one can infer that the thermal waves in the rotating nanobeam are smooth and continuous functions and reach the steady-state response along with the distance of the nano-beam. This is in good agreement with the experimental and physical points of view, since the amount of heat is reduced with the reversal of the heat waves propagation. Furthermore, in the presence of the non-locality effect ($\bar{\xi} = 1$ and $\bar{\xi} = 3$), the magnitude of θ is somehow smaller than those in the absence of non-locality effect ($\bar{\xi} = 0$). This demonstrates the difference between the generalized local thermoelasticity and non-local generalized models of thermoelasticity. The effect of non-local term is to decrease the temperature distribution. Generally speaking, this parameter has a weak influence on the distribution of temperature compared to other field variables.

The variation of the non-dimensional axial displacement u versus x for local and nonlocal theories are depicted in Figure 5. It can be seen that any increase in the value of $\bar{\xi}$ causes an increase in the amount of the negative displacements of u when $0 \leq x \leq 0.44$ and increases the positive values of u in the interval $0.44 \leq x \leq 1.0$. By reducing the rigidity of nanobeam, the non-local effect yields the higher values of transverse and axial displacements. As a result, the nonlocal nanobeam is more flexible than the classical one.

The distribution of the bending moment M in terms of distance x based on the classical and non-local models are plotted in Figure 6. It is also noted that as distance x moves forward, the bending moment M decreases. Furthermore, any increase in $\bar{\xi}$ results in the greater values for nonlocal bending moments. One can infer that the nonlocality of nanobeam will significantly changes the thermomechanical behavior of the structure, especially its mechanical features, and therefore it is very important to consider it in designing of spinning nanobeams.

7.3 The impact of angular speed of the nanobeam

The effect of angular speed Ω on the nondimensional field vectors has been presented in this subsection. The vibrational behavior of the rotating nanobeams is influenced by the rotating speed Ω. Figures 7-10 are presented to demonstrate this effect. It is assumed that the velocity of moving load $\bar{v}$, the phase lags τ_q and τ_θ, the nonlocal parameter $\bar{\xi}$ and the ramping time t_0 are fixed and take the values ($\bar{v} = 1, \tau_q = 0.05, \tau_\theta = 0.02, t_0 = 0.1,$ and $\bar{\xi} = 1$). Three different values of angular speed

($\Omega = 0, 0.1, 0.3$) are chosen to investigate the impact of this parameter on the mechanical behavior of the rotating nanobeam. As a special case study and in the absence of angular velocity, the rotation speed is assumed to be zero ($\Omega = 0$). As the results of this section are compared to those for other parameters, it is concluded the vibrational response of the system are considerably affected by parameter Ω. Moreover, the distance r between the left edge of the nanobeam and the spinning axis has a great influence on the variation of the field variables.

Figure 7 displays the influence of rotation on the transverse deflection w. The figure shows that the angular velocity Ω reduces the deflection w. It is concluded that the nanobeam becomes stiffer in the presence of angular rotation. These findings are in good agreement with those reported by Ebrahimi and Haghi [80]. The variation of temperature θ at any axial point x is examined in Fig. 8 for three values of angular speed. One concludes that as Ω increases, the temperature distribution also shifts upward. Furthermore, the figure shows the slight influence of the rotation speed on the temperature distribution which are consistent with the results obtained by previous works [81, 82]. Figure 9 presents the impact of parameter Ω on the variation of axial displacement u. It is revealed that the impact of angular velocity Ω is to decrease the absolute values of displacement u. Finally, according to Fig. 10, one observes that in the presence of angular velocity, the bending moment M is slightly increased.

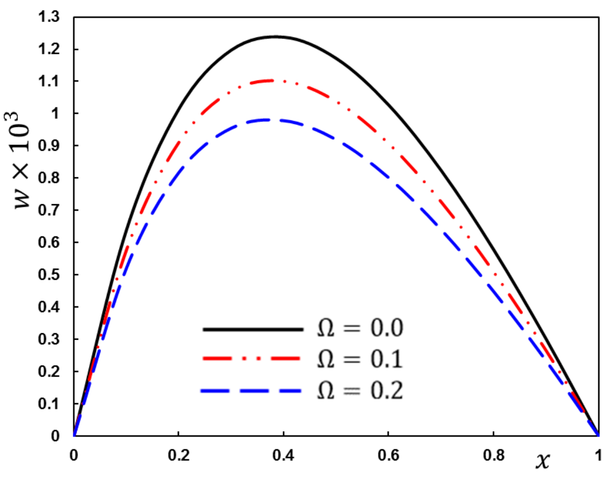

Figure 7: The variation of deflection w versus x for some assigned values of rotation speed Ω

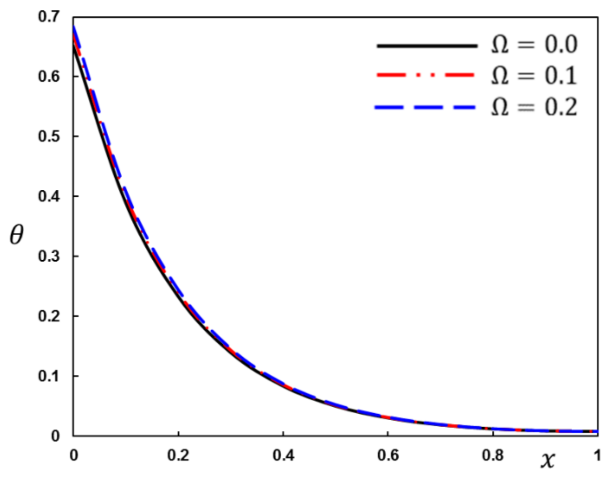

Figure 8: The variation of temperature θ vs x for some assigned values of rotations speed Ω

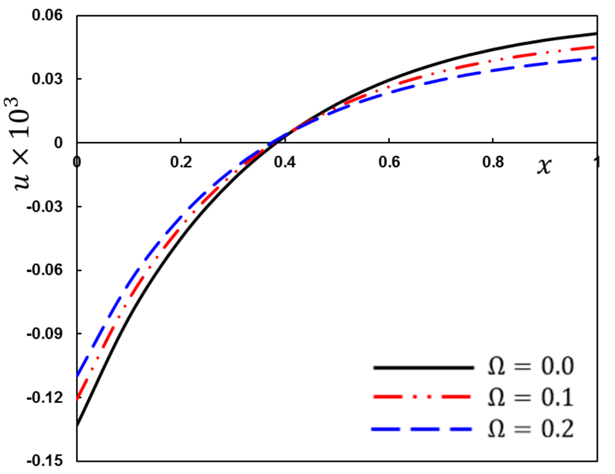

Figure 9: The variation of displacement u vs x for some assigned values of rotations speed Ω

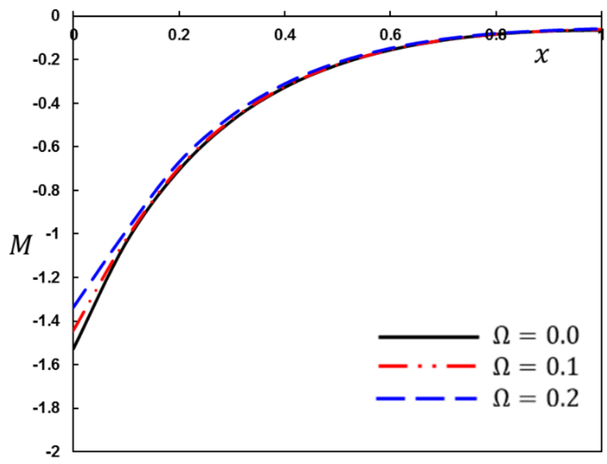

Figure 10: The variation of bending moment M vs x for some assigned values of rotations speed Ω

It is finally exhibited that the thermomechanical behavior of rotating micromachined beams is very sensitive to the values of rotational speed and therefore the results of this section provide useful theoretical findings to precisely design the blades of miniaturized turbines [80, 83, 84].

7.4 The impact of moving load velocity

In the previous studies, many researchers have modeled and discussed the problem of small-scale systems in the presence of moving load by employing nonlocal theory of elasticity. However, this problem has not yet been discussed thoroughly on how nonlocal stress theories are affected by moving load velocity. Figures 11-14 show the distributions of field variables for some assigned values of moving load velocity. In order to justify the integrity of the present results, the simulations are performed by considering the microbeam parameters reported in the literature [85, 86]. It may be determined that the mechanical behavior of rotating nanobeam is more sensitive to the influence of moving load velocity compared to its thermal characteristics. More specifically, the velocity of moving load has no effect on the temperature distribution.

In this section, the angular velocity Ω, nonlocal parameter $\bar{\xi}$, the ramping time t_0, the phase lags τ_q and τ_θ are supposed to be fixed and take the values ($\Omega = 0.1, \tau_q = 0.05, \tau_\theta = 0.02, t_0 = 0.1$, and $\bar{\xi} = 1$). According to the illustrated results, it is evident that parameter $\bar{\upsilon}$ plays a key role in the vibrational response of the system. The variation of transverse deflection w against the axial velocity is shown in Figure 11. It is clear that with by increasing the moving load velocity $\bar{\upsilon}$, the non-dimensional deflection w decreases which is consistent with practical findings in the literature.

Figure 12 shows the effect of parameter $\bar{\upsilon}$ on the temperature distribution θ in the case of nonlocal elasticity theory. According to this figure, it is evident that the moving load velocity has no influence on the temperature gradient θ. This important observation is in coincidence with those obtained by Abouelregal and Zenkour [42], as for the absence of rotation.

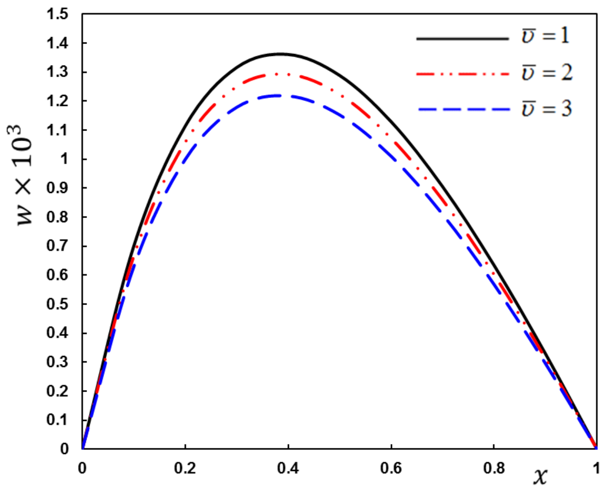

Figure 11: The distribution of deflection w vs x for some assigned values of speed $\bar{\upsilon}$

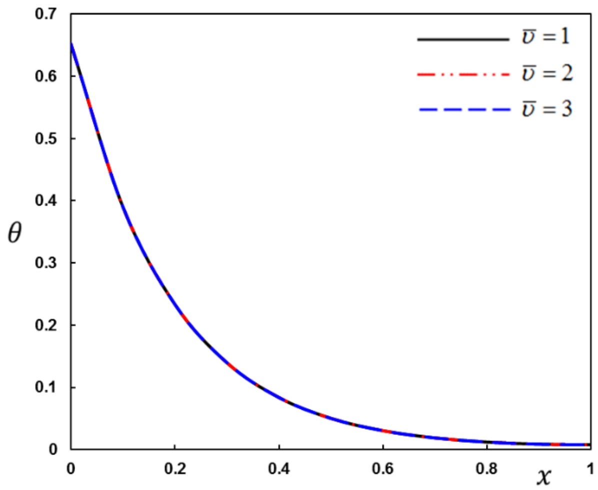

Figure 12: The distribution of temperature θ vs x for some assigned values of speed $\bar{\upsilon}$

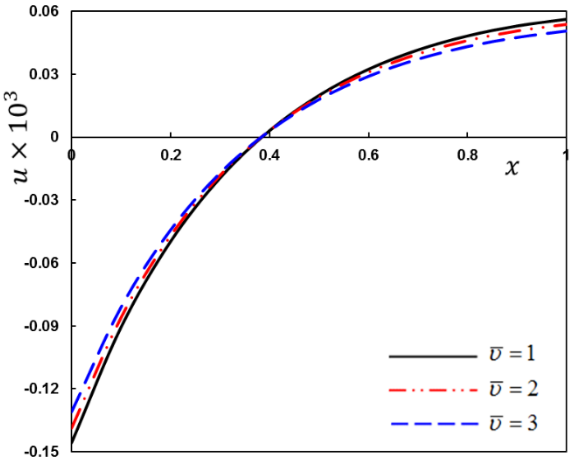

Figure 13: The distribution of displacement u vs x for some assigned values of speed $\bar{\upsilon}$

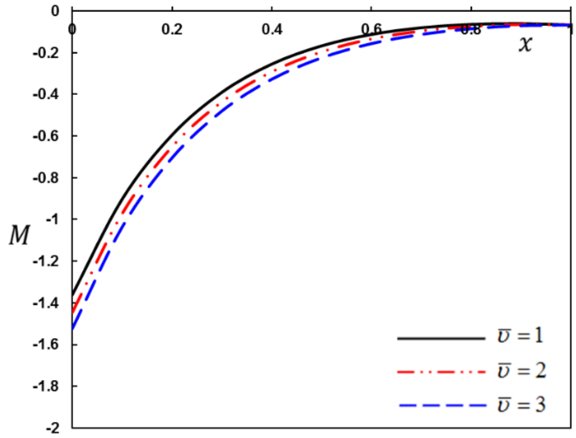

Figure 14: The distribution of bending moment M vs x for some assigned values of speed $\bar{\upsilon}$

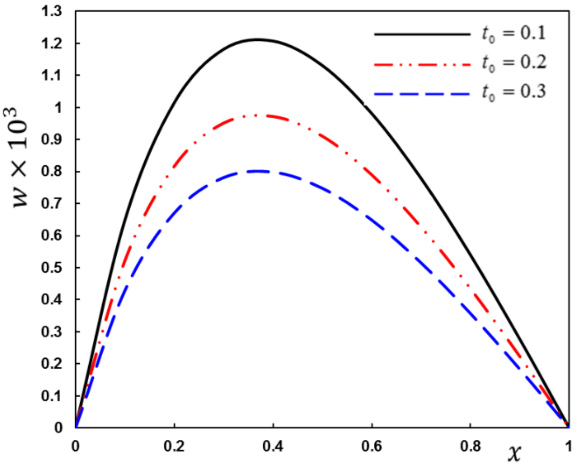

Figure 15: The distribution of deflection w for some assigned values of ramping time t_0

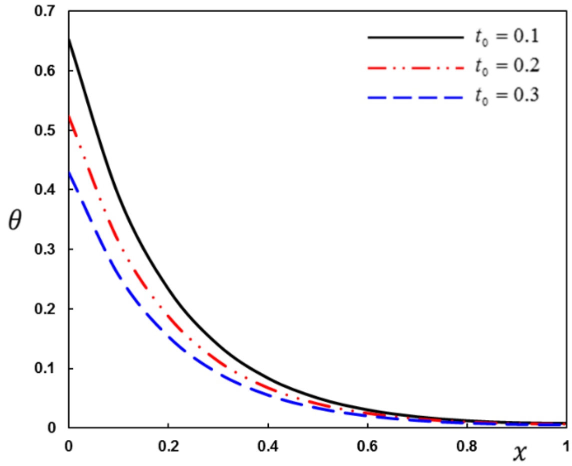

Figure 16: The distribution of temperature θ for some assigned values of ramping time t_0

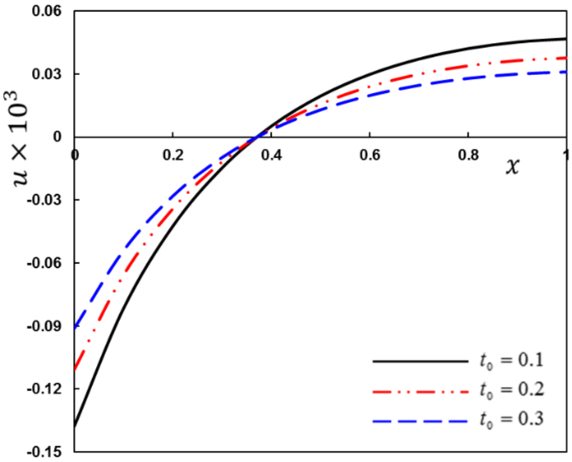

Figure 17: The distribution of displacement u for some assigned values of ramping time t_0

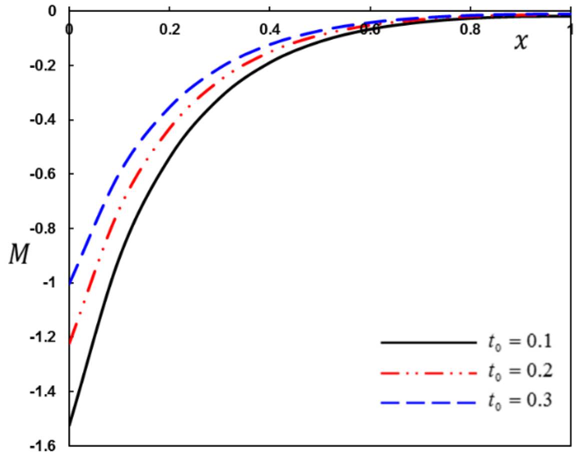

Figure 18: The distribution of bending moment M for some assigned values of ramping time t_0

Figure 13 is displayed to analyze the effect of moving load velocity $\bar{v}$ on the axial displacement u. It is indicated that the values of the absolute values of displacement u intend to decrease as the loading velocity is taken into account. Finally, Fig. 14 demonstrates the variation of the flexural moment M for three valued of moving load velocity $\bar{v}$. One can deduce that the effect of the parameter $\bar{v}$ is to increase the flexural moment M. Generally speaking, it can be concluded that, in the presence of loading velocity, the absolute values of transverse and axial displacements becomes smaller and the bending moment shifts upward by considering the loading velocity $\bar{v}$.

7.5 The impact of ramping time

In the current subsection, the effect of ramping time t_0 on the vibration behavior and temperature distribution is investigated by considering the variation of transverse and axial deflections, thermal and flexural moment distributions with the aid of thermal load expression defined in Eq. (42). The capacity of components and systems to resist against the variation of environmental temperature is very crucial in designing the sensitive devices like microelectromechanical systems in real-world applications. To determine the ramping time in experimental testing, the set point temperature is progressively increased by ramp heating, which helps to minimize the thermal shock. Thermal shock happens when heat causes various parts of an item to expand at different rates.

In this section, the phase lags τ_q and τ_θ, the angular velocity Ω, the nonlocal parameter $\bar{\xi}$ and the moving load velocity $\bar{v}$ are considered to be constant. The obtained results are illustrated through Figs. 15-18. The following observations are extracted:

1- The ramping time t_0 has a considerable influence on the distributions of different system parameters.
2- The presence of ramping time is found to have a considerable impact on the reduction of non-dimensional deflections.
3- Any increase in the ramping time leads to a decrease in the lateral vibration w and temperature gradient θ, which is evident in Figures 15 and 16.
4- As can be seen in Figure 17, the absolute values of axial displacement u are decreased in the presence of ramping time t_0.
5- Any increase in the values of parameter t_0 results in decreasing the bending moment M, as can be observed from Figure 18.
6- For aerospace constructions, the temperature ramp rate is important for modelling the practical temperature changes.

7.6 A comparative study on different thermoelasticity models

The final case explores how the non-dimensional physical fields are affected by the heat flux delay τ_q and the temperature gradient delay τ_θ while the other system parameters remain constant. The transverse deflection, thermodynamic temperature, bending moment and axial displacement of the rotating nanobeam are illustrated in Figures 19-22 for the sake of comparison between the results of different theories. The coupling theory of thermoelasticity (CTE) can be obtained when $\tau_q = \tau_\theta = 0$ and the Lord-Shulman (LS) model is available when $\tau_q = 0.05 > 0$ and $\tau_\theta = 0$. The dual-phase lag theory (DPL) proposed by Tzou and in its generalized form, can be achieved by considering $\tau_q = 0.0$ and $\tau_\theta = 0.02$.
From the illustrated results of this section, one can figure out that:

- The delay parameters τ_q and τ_θ have a pronounced influence on the distribution of all field variables.
- The trends of the obtained results for the coupled (CTE) and generalized thermoelastic models (LS and DPL) are almost identical and their values are different.
- Compared to CTE theory, the values of temperature distributions in LS and DPL models are smaller.

- By considering LS and DPL theories, the absolute values of transverse and axial displacements as well as bending moment are smaller compared to CTE theory.

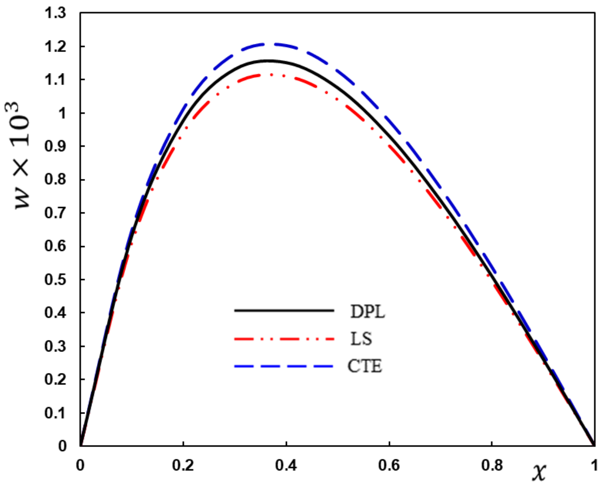

Figure 19: The distribution of deflection w for different models of thermoelasticity

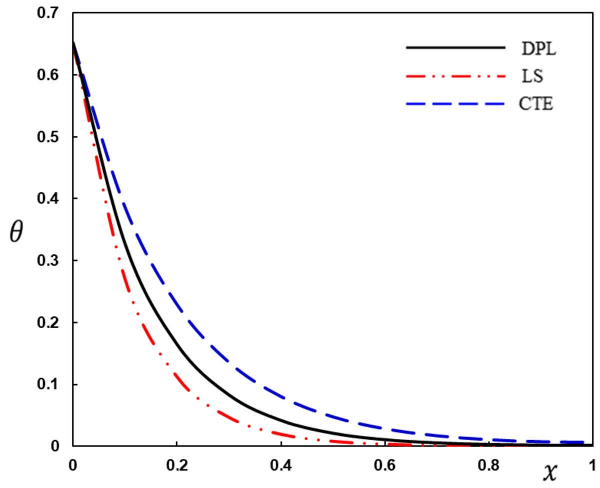

Figure 20: The distribution of temperature θ for different models of thermoelasticity

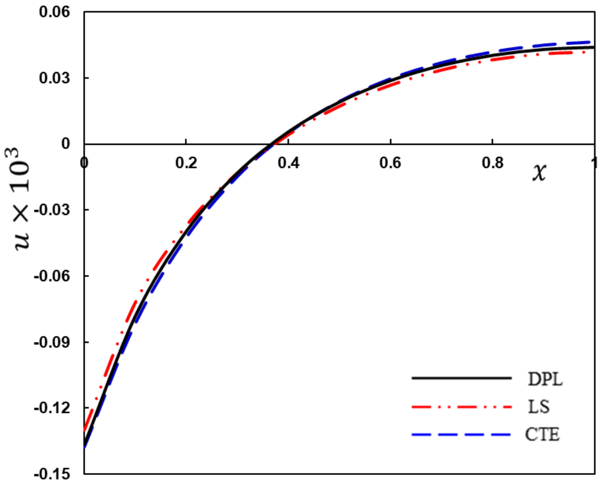

Figure 21: The distribution of displacement u for different models of thermoelasticity

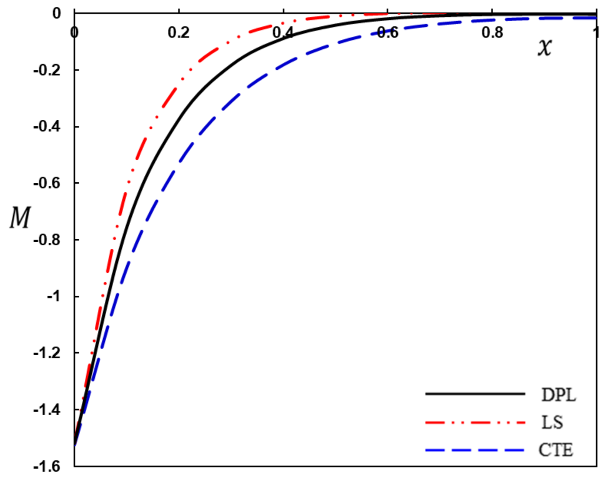

Figure 22: The distribution of moment M for different models of thermoelasticity

8. Conclusion

The current work was aimed at investigating the size-dependent mechanical and thermal characteristics of rotating nanobeams. To this end, on the basis of non-local elasticity theory in conjunction with the generalized thermoelasticity theory, including phase delays, the basic equations governing the motion of nanobeams under a constant-velocity moving load were presented. The performance of rotating micromachined structures like miniaturized turbine blades strongly depends on the thermomechanical behavior of their components. By considering the simply-supported end conditions and employing the Laplace transform technique, the analytical solutions were found and the impacts of moving load velocity and angular speed on the distributions of field variables were theoretically studied. Furthermore, the effects of ramping time rate of thermal load and nonlocality were thoroughly investigated. It was shown that the results of the proposed model are in agreement with those reported in the literature. It was demonstrated that, due to the small-scale effects, the dynamic deflection of nanobeam are often higher than those of classical theory. Moreover, it was revealed that the behavior of nanoscale beams significantly depends on the ramping time of the thermal load. It was finally concluded that the moving load velocity has no effect on the temperature distribution and the non-local parameter has a slight effect on the thermal behavior of the system. By considering LS and DPL theories, the absolute values of different field variables were smaller compared to CTE theory.

Disclosure statement

No potential conflict of interest was reported by the authors.

Funding

H. M. Sedighi is grateful to the Research Council of Shahid Chamran University of Ahvaz for its financial support (Grant No. SCU.EM1400.98).

V. A. Eremeyev acknowledges the support of the Government of the Russian Federation (contract No. 14.Z50.31.0046).

ORCID iD

Ahmed E. Abouelregal https://orcid.org/0000-0003-3363-7924
Hamid M. Sedighi https://orcid.org/0000-0002-3852-5473
Mohammad Malikan https://orcid.org/0000-0001-7356-2168
Victor A. Eremeyev https://orcid.org/0000-0002-8128-3262

References

[1] Thai, HT. Nonlocal continuum field theories. New York, NY: Springer, 2002.
[2] Safarabadi,M, Mohammadi, M, Farajpour A, and Goodarzi, M. Effect of surface energy on the vibration analysis of rotating nanobeam. J Solid Mech 2015; 7(3): 299-311.
[3] Ghayesh, M. H. (2018). Nonlinear Vibrations of Axially Functionally Graded Timoshenko Tapered Beams. Journal of Computational and Nonlinear Dynamics, 13(4), 041002.
[4] Ghayesh, M. H. (2019). Nonlinear oscillations of FG cantilevers. Applied Acoustics, 145, 393–398.
[5] Ghayesh, M. H. (2019). Asymmetric viscoelastic nonlinear vibrations of imperfect AFG beams. Applied Acoustics, 154, 121–128.
[6] Ghayesh, M. H. (2019). Viscoelastic mechanics of Timoshenko functionally graded imperfect microbeams. Composite Structures, 225, 110974.
[7] Ghayesh, M. H. Mechanics of viscoelastic functionally graded microcantilevers. European Journal of Mechanics-A/Solids, 73, 2019, 492-499.
[8] Ghayesh, M. H. (2019). Viscoelastic dynamics of axially FG microbeams. International Journal of Engineering Science, 135, 75–85.
[9] Ghayesh, M. H. (2018). Nonlinear dynamics of multilayered microplates. Journal of Computational and Nonlinear Dynamics, 13(2), 021006-1.
[10] Ouakad HM, Valipour A, Żur KK, Sedighi HM, Reddy JN. On the nonlinear vibration and static deflection problems of actuated hybrid nanotubes based on the stress-driven nonlocal integral elasticity. Mechanics of Materials. 2020; 148: 103532.
[11] Koochi, A., & Goharimanesh, M. (2021). Nonlinear Oscillations of CNT Nano-resonator Based on Nonlocal Elasticity: The Energy Balance Method. Reports in Mechanical Engineering, 2(1), 41-50.
[12] Mindlin, R.D., Eshel, N.N. On first strain-gradient theories in linear elasticity. Int J Solids Struct 1968; 4(1): 109–124.
[13] Soltani D, Akbarzadeh Khorshidi M, Sedighi HM. Higher order and scale-dependent micro-inertia effect on the longitudinal dispersion based on the modified couple stress theory. Journal of Computational Design and Engineering. 2021; 8(1):189-94.
[14] Wang, C.Y., Murmu, T., Adhikari, S. Mechanisms of nonlocal effect on the vibration of nanoplates. Appl Phys Lett 2011; 98(15) 153101.
[15] Abouelregal, A.E., Marin, M. The size-dependent thermoelastic vibrations of nanobeams subjected to harmonic excitation and rectified sine wave heating. Mathematics 2020; 8(7): 1128.
[16] Sedighi HM, Ouakad HM, Dimitri R, Tornabene F. Stress-driven nonlocal elasticity for the instability analysis of fluid-conveying C-BN hybrid-nanotube in a magneto-thermal environment. Physica Scripta. 2020; 95(6): 065204.
[17] Sedighi HM, Malikan M. Stress-driven nonlocal elasticity for nonlinear vibration characteristics of carbon/boron-nitride hetero-nanotube subject to magneto-thermal environment. Physica Scripta. 2020; 95(5): 055218.

[18] Rysaeva LK, Korznikova EA, Murzaev RT, Abdullina DU, Kudreyko AA, Baimova JA, Lisovenko DS, Dmitriev SV. Elastic damper based on the carbon nanotube bundle. Facta Universitatis Series-Mechanical Engineering. 2020; 18(1): 001-12.
[19] Abouelregal, A.E., Mohammed, W.W. Effects of nonlocal thermoelasticity on nanoscale beams based on couple stress theory. Math Meth App Sci, 2020; https://doi.org/10.1002/mma.6764.
[20] Abouelregal AE, Mohammad-Sedighi H, Faghidian SA, Shirazi AH. TEMPERATURE-DEPENDENT PHYSICAL CHARACTERISTICS OF THE ROTATING NONLOCAL NANOBEAMS SUBJECT TO A VARYING HEAT SOURCE AND A DYNAMIC LOAD. Facta Universitatis Series-Mechanical Engineering. 2021, doi: 10.22190/FUME201222024A.
[21] Barati, M.R., Shahverdi, H. Small-scale effects on the dynamic response of inhomogeneous nanobeams on elastic substrate under uniform dynamic load. Eur Phys J Plus 2017; 132(4) 167.
[22] Abouelregal A.E., Marin M. The response of nanobeams with temperature-dependent properties using state-space method via modified couple stress theory. Symmetry 2020; 12(8): 1276.
[23] Xu, X.J., Zheng, M.L., Wang, X.C. On vibrations of nonlocal rods: Boundary conditions, exact solutions and their asymptotics. Int J Eng Sci 207; 119: 217–231.
[24] Sharma R, Raju CS, Animasaun IL, Santhosh HB, Mishra MK. Insight into the significance of Joule dissipation, thermal jump and partial slip: Dynamics of unsteady ethelene glycol conveying graphene nanoparticles through porous medium. Nonlinear Engineering. 2021; 10(1): 16-27.
[25] Abouelregal, A.E., Mohamed, B.O. Fractional order thermoelasticity for a functionally graded thermoelastic nanobeam induced by a sinusoidal pulse heating. J Comput Theor Nanosci 2018; 15: 1233–1242.
[26] Sari, M.S., Al-Kouz, W.G., Atieh, A.M. Transverse vibration of functionally graded tapered double nanobeams resting on elastic foundation. Appl Sci 2020; 10: 493.
[27] Chandel, V.S., Wang, G., Talha, M. Advances in modelling and analysis of nano structures: a review, Nanotechnol Rev 2020; 9: 230–258.
[28] Hosseini-Hashemi, S., Behdad, S., Fakher, M. Vibration analysis of two-phase local/nonlocal viscoelastic nanobeams with surface effects. Eur Phys J Plus 2020; 135: 190.
[29] Malikan, M., Eremeyev, V. A. On the Dynamics of a Visco–Piezo–Flexoelectric Nanobeam. Symmetry 2020; 12: 643. https://doi.org/10.3390/sym12040643
[30] Malikan, M., Eremeyev, V. A., Sedighi, H. M. Buckling analysis of a non-concentric double-walled carbon nanotube. Acta Mech 2020; 231: 5007–5020. https://doi.org/10.1007/s00707-020-02784-7
[31] Malikan, M., Uglov, N. S., Eremeyev, V. A. On instabilities and post-buckling of piezomagnetic and flexomagnetic nanostructures. Inter J Eng Sci, 2020; 157: 103395.
[32] Konobeeva NN, Belonenko MB. Influence of a magnetic field on the propagation of ultrashort optical pulses in anisotropic optical media with carbon nanotubes. NANOSYSTEMS: PHYSICS, CHEMISTRY, MATHEMATICS. 2021; 12(4): 430-5.
[33] A. H. Sofiyev, Dynamic buckling of functionally graded cylindrical shells under non-periodic impulsive loading. Acta Mechanica, 2003; 165: 151-163.
[34] Sofiyev, A. H. Dynamic response of an FGM cylindrical shell under moving loads. Composite Structures, 2010; 93(1): 58–66.
[35] Alizada, A. N., Sofiyev, A. H., and Kuruoglu, N. Stress analysis of a substrate coated by nanomaterials with vacancies subjected to uniform extension load. Acta Mechanica, 2012; 223(7): 1371–1383.
[36] Avey, M., and Yusufoglu, E. On the solution of large-amplitude vibration of carbon nanotube-based double-curved shallow shells. Mathematical Methods in the Applied Sciences, 2020; 1–13. https://doi.org/10.1002/mma.6820
[37] Sofiyev, A. H., Avey, M., and Kuruoglu, N. An approach to the solution of nonlinear forced vibration problem of structural systems reinforced with advanced materials in the presence of viscous damping. Mechanical Systems and Signal Processing, 2021; 161, 107991.
[38] Sofiyev, A., Bayramov, R. P. oglu, and Heydarov, S. H. oglu. The forced vibration of infinitely long cylinders reinforced by carbon nanotubes subjected to combined internal and ring-shaped compressive pressures. Mathematical Methods in the Applied Sciences. 2020; doi:10.1002/mma.6610
[39] Pham, P.T., Hong, K.S. Dynamic models of axially moving systems: A review. Nonlinear Dyn 2020; 31: 1–35.
[40] Marynowski, K., Kapitaniak, T. Dynamics of axially moving continua. Int J Mech Sci 2014; 81: 26–41.
[41] Zenkour A.M., Abouelregal, A.E. Decaying temperature and dynamic response of a thermoelastic nanobeam to a moving load. Advan Comput Des 2018; 3(1): 1-16.
[42] Abouelregal, A.E., Zenkour, A.M. Dynamic response of a nanobeam induced by ramp-type heating and subjected to a moving load. Microsyst Technol 2017; 23(12): 5911-5920.
[43] Arda, M. Vibration Analysis of an Axially Loaded Viscoelastic Nanobeam. Int J Eng Appl Sci 2018; 10(3): 252-263.
[44] Lin, Y.H., Trethewey, M.W. Finite element analysis of elastic beams subjected to moving dynamic loads. J Sound Vibr 1990; 136(2): 323–342.
[45] Shariati A, Mohammad-Sedighi H, Żur KK, Habibi M, Safa M. On the vibrations and stability of moving viscoelastic axially functionally graded nanobeams. Materials. 2020; 13(7): 1707.

[46] Jaiswal, O.R., Iyengar, R.N. Dynamic response of a beam on elastic foundation of finite depth under a moving force. Acta Mech 1993; 96: 67–83.
[47] Lee, H.P. Dynamic response of a beam with intermediate point constraints subjected to a moving load. J Sound Vibr 1994; 171(3): 361–368.
[48] http://www.ritsumei.ac.jp/se/~sugiyama/research/re_2.3e%27.html
[49] Andolfatto, L. et al., Simulation of energy recovery on water utility networks by a micro-turbine with counter-rotating runners. IOP Conf. Series: Earth and Environmental Science 2016; 49: 102012.
[50] Xia, D., Yu, C., Kong, L. The Development of Micromachined Gyroscope Structure and Circuitry Technology. Sensors 2014; 14: 1394-1473.
[51] Hosseini M, Shishesaz M, Tahan KN, Hadi A. Stress analysis of rotating nano-disks of variable thickness made of functionally graded materials. International Journal of Engineering Science. 2016; 109: 29-53.
[52] Mohammadi, M., Safarabadi, M., Rastgoo, A., Farajpour, A. Hygro-mechanical vibration analysis of a rotating viscoelastic nanobeam embedded in a visco-Pasternak elastic medium and in a nonlinear thermal environment. Acta Mech 2016; 227(8): 2207–2232.
[53] Hosseini M, Shishesaz M, Hadi A. Thermoelastic analysis of rotating functionally graded micro/nanodisks of variable thickness. Thin-Walled Structures. 2019; 134: 508-23.
[54] Ebrahimi, F., Dabbagh, A. Wave propagation analysis of smart rotating porous heterogeneous piezo-electric nanobeams. Eur Phy J Plus 2017; 132(4): 153.
[55] Khadimallah MA, Hussain M, Elbahar M, Ghandourah E, Elimame E, Tounsi A. The effects of ring and fraction laws: Vibration of rotating isotropic cylindrical shell. Advances in nano research. 2021; 11(1): 19-26.
[56] Karimi-Nobandegani A, Fazelzadeh SA, Ghavanloo E. Flutter instability of cracked rotating non-uniform beams subjected to distributed follower force. International Journal of Structural Stability and Dynamics. 2018; 18(01): 1850001.
[57] Zhang, S., Liu, W.K., Ruo, R.S. Atomistic Simulations of Double-Walled Carbon Nanotubes (DWCNTs) as Rotational Bearings. Nano Lett 2004; 4: 293.
[58] Ghommem M, Abdelkefi A. Nonlinear analysis of rotating nanocrystalline silicon microbeams for microgyroscope applications. Microsystem Technologies. 2017; 23(12): 5931-46.
[59] Ghayesh MH, Farokhi H, Alici G. Size-dependent performance of microgyroscopes. International Journal of Engineering Science. 2016; 100: 99-111.
[60] Apuzzo A, Barretta R, Canadija M, Feo L, Luciano R, de Sciarra FM. A closed-form model for torsion of nanobeams with an enhanced nonlocal formulation. Composites Part B: Engineering. 2017; 108: 315-24.
[61] Abouelregal, A.E. Modified fractional photo-thermoelastic model for a rotating semiconductor half-space subjected to a magnetic field. Silicon (2020); https://doi.org/10.1007/s12633-020-00380-x
[62] Yahya AM, Abouelregal AE, Khalil KM, Atta D. Thermoelastic responses in rotating nanobeams with variable physical properties due to periodic pulse heating. Case Studies in Thermal Engineering. 2021; 28: 101443.
[63] Biot, M.A. Thermoelasticity and irreversible thermodynamics. J Appl Phys 1956; 27 (3): 240–53.
[64] Lord, H.W., Shulman, Y. A generalized dynamical theory of thermoelasticity. J Mech Phys Solids 1967; 15(5): 299–309.
[65] Tzou, D.Y. A unified approach for heat conduction from macro-to micro-scales. J Heat Transfer 1995; 117: 8–16.
[66] Tzou, D.Y. Macro- to micro-scale heat transfer: The lagging behavior. Abingdon: Taylor & Francis, 1997.
[67] Tzou, D.Y. Experimental support for the Lagging behavior in heat propagation. J Thermophysics Heat Transfer 1995; 9: 686–693.
[68] Abouelregal, A.E. Modified fractional thermoelasticity model with multi-relaxation times of higher order: Application to spherical cavity exposed to a harmonic varying heat. Wav Rand Compl Media 2019; 1–21. doi:10.1080/17455030.2019.1628320
[69] Abouelregal, A.E. Two-temperature thermoelastic model without energy dissipation including higher order time-derivatives and two phase-lags. Mater Research Express 2019; 6(11): 116535.
[70] Abouelregal AE, Mohammed WW, Mohammad-Sedighi H. Vibration analysis of functionally graded microbeam under initial stress via a generalized thermoelastic model with dual-phase lags. Archive of Applied Mechanics. 2021; 91(5): 2127-42.
[71] Abouelregal, A.E. A novel generalized thermoelasticity with higher-order time-derivatives and three-phase lags. Multidiscip Model Mater Struct 2019; 16(4): 689-711.
[72] Abouelregal, A.E. Three-phase-lag thermoelastic heat conduction model with higher-order time-fractional derivatives. Indian J Phys (2019); https://doi.org/10.1007/s12648-019-01635-z.
[73] Abouelregal, A.E, Yao, S.W., Ahmad, H. Analysis of a functionally graded thermopiezoelectric finite rod excited by a moving heat source. Results Physics 2020; doi: https://doi.org/10.1016/j.rinp.2020.103389.
[74] Danesh, H., Javanbakht, M., Mohammadi Aghdam, M. A comparative study of 1D nonlocal integral Timoshenko beam and 2D nonlocal integral elasticity theories for bending of nanoscale beams. Continuum Mech Thermodyn (2021). https://doi.org/10.1007/s00161-021-00976-7
[75] Roghani, M., Rouhi, H. Nonlinear stress-driven nonlocal formulation of Timoshenko beams made of FGMs. Continuum Mech Thermodyn (2020). https://doi.org/10.1007/s00161-020-00906-z

[76] Romano, G., Luciano, R., Barretta, R. et al. Nonlocal integral elasticity in nanostructures, mixtures, boundary effects and limit behaviours. Continuum Mech Thermodyn 2018; 30, 641–655. https://doi.org/10.1007/s00161-018-0631-0
[77] Roudbari, M.A., Ansari, R. Single-walled boron nitride nanotube as nano-sensor. Continuum Mech. Thermodyn 2020; 32, 729–748. https://doi.org/10.1007/s00161-018-0719-6
[78] Inan, E., Eringen, A.C. Nonlocal theory of wave propagation in thermoelastic plates. Int J Eng Sc 1991; 29: 831-843.
[79] Bachher, M., Sarkar N. Nonlocal theory of thermoelastic materials with voids and fractional derivative heat transfer. Wav Rand Compl Media 2019; 29(4): 595-613.
[80] Ebrahimi, F, Haghi, P. Elastic wave dispersion modelling within rotating functionally graded nanobeams in thermal environment. Advanc Nano Research 2018; 6(3): 201-217.
[81] Shafiei, N., Kazemi, M., Ghadiri, M. Comparison of modeling of the rotating tapered axially functionally graded Timoshenko and Euler–Bernoulli microbeams. Phys E: Low dimen Sys Nanostruct 2016; 83: 74-87.
[82] Younesian, D., Esmailzadeh, E. Vibration suppression of rotating beams using time varying internal tensile force. J Sound Vibrat 2011; 330(2), 308-320.
[83] Khaniki, H.B. Vibration analysis of rotating nanobeam systems using Eringen's two-phase local/nonlocal model. Phys E: Low dimen Sys Nanostruct 2018; 99: 310–319.
[84] Fang, J., Gu, J., Wang, H. Size-dependent three-dimensional free vibration of rotating functionally graded microbeams based on a modified couple stress theory. Int J Mech Sci 2018; 136, 188-199.
[85] Esen, I. Dynamics of size-dependent Timoshenko microbeams subjected to moving loads. Int J Mech Sci 2020; 175: 105501.
[86] Yas, M.H., Heshmati, M. Dynamic analysis of functionally graded nanocomposite beams reinforced by randomly oriented carbon nanotube under the action of moving load. Appl Math Model, 2012; 36: 1371–1394.